Cellular hysteresis as a principle to maximize the efficacy of antibiotic therapy

Roderich Roemhild[a,b], Chaitanya S. Gokhale[a], Philipp Dirksen[a,b], Christopher Blake[b], Philip Rosenstiel[c], Arne Traulsen[a], Dan I. Andersson[d], and Hinrich Schulenburg[a,b,1]

[a]Antibiotic Resistance Evolution Group, Max-Planck-Institute for Evolutionary Biology, 24306 Plön, Germany; [b]Department of Evolutionary Ecology and Genetics, Zoological Institute, Christian-Albrechts-Universität zu Kiel, 24118 Kiel, Germany; [c]Institute of Clinical Molecular Biology, Universitätsklinikum Schleswig-Holstein, 24105 Kiel, Germany; and [d]Department of Medical Biochemistry and Microbiology, Uppsala University, SE- 751 23 Uppsala, Sweden

Edited by Shimon Bershtein, Ben-Gurion University, Beer-Sheva, Israel, and accepted by Editorial Board Member Daniel L. Hartl August 16, 2018 (received for review June 10, 2018)

Antibiotic resistance has become one of the most dramatic threats to global health. While novel treatment options are urgently required, most attempts focus on finding new antibiotic substances. However, their development is costly, and their efficacy is often compromised within short time periods due to the enormous potential of microorganisms for rapid adaptation. Here, we developed a strategy that uses the currently available antibiotics. Our strategy exploits cellular hysteresis, which is the long-lasting, transgenerational change in cellular physiology that is induced by one antibiotic and sensitizes bacteria to another subsequently administered antibiotic. Using evolution experiments, mathematical modeling, genomics, and functional genetic analysis, we demonstrate that sequential treatment protocols with high levels of cellular hysteresis constrain the evolving bacteria by (*i*) increasing extinction frequencies, (*ii*) reducing adaptation rates, and (*iii*) limiting emergence of multidrug resistance. Cellular hysteresis is most effective in fast sequential protocols, in which antibiotics are changed within 12 h or 24 h, in contrast to the less frequent changes in cycling protocols commonly implemented in hospitals. We found that cellular hysteresis imposes specific selective pressure on the bacteria that disfavors resistance mutations. Instead, if bacterial populations survive, hysteresis is countered in two distinct ways, either through a process related to antibiotic tolerance or a mechanism controlled by the previously uncharacterized two-component regulator CpxS. We conclude that cellular hysteresis can be harnessed to optimize antibiotic therapy, to achieve both enhanced bacterial elimination and reduced resistance evolution.

experimental evolution | antibiotic resistance | *Pseudomonas aeruginosa* | cellular hysteresis | sequential treatment

Natural environments are often temporally dynamic. They produce continuously changing selective constraints that are a particular challenge for organisms to adapt to (1). Similar dynamic conditions may be used in human therapy to limit the ability of pathogens for resistance evolution. Antibiotic resistance is a global threat (2), enhanced by the ongoing emergence of new resistance mechanisms (3, 4). Sequential treatments may be one option to counter emerging resistance: The alternation of antibiotics may produce the challenging selection conditions that are known from many fluctuating natural environments. Indeed, previous evolution experiments consistently identified reduced resistance evolution and increased extinction at sublethal drug concentrations in sequential treatment protocols (5–8). The efficacy of sequential treatments has generally been attributed to the evolution of collateral sensitivity (9, 10), i.e., genetic trade-offs. Collateral sensitivity describes the case where resistance mutations pleiotropically increase sensitivity to other antibiotics. Intriguingly, collateral sensitivity only occasionally explains the observed dynamics of resistance evolution (5), indicating the activity of unknown selective pressures.

An alternative selective pressure may be caused by antibiotic-induced physiological changes in bacterial cells. Such inducible changes can affect motility (11), biofilm formation (12), and heat shock response (13). Moreover, certain bacterial responses can be stabilized across generations. For example, the lactose utilization response in *Escherichia coli* is maintained for >10 generations after removal of lactose, by the inheritance of stable proteins (14). Positive autoregulation, a common feature of two-component sensors, can similarly stabilize responses for several days, as observed with PhoQ/PhoP (15). Upon specific environmental change, these inherited responses can have deleterious fitness effects. For example, salt-induced expression of the PhoE porin increases sensitivity to acid (16). Furthermore, structural damage from past stress encounters may be amplified in new environments. We here use the term "cellular hysteresis" (17) to summarize the inducible and long-lasting physiological effects on cellular integrity and function, spanning both discrete and quantitative changes. The term is more general than phenotypic memory, as it comprises positive and negative fitness effects induced by previous exposures. Although cellular hysteresis likely determines pathogen survival during sequential antibiotic treatments, it is not part of current treatment concepts. Consideration of negative hysteresis may enhance treatment efficacy when exposure to one antibiotic temporarily increases susceptibility to a subsequently administered second antibiotic.

Significance

Rapid evolution is central to the current antibiotic crisis. Sustainable treatments must thus take account of the bacteria's potential for adaptation. We identified cellular hysteresis as a principle to constrain bacterial evolution. Cellular hysteresis is a persistent change in bacterial physiology, reminiscent of cellular memory, which is induced by one antibiotic and enhances susceptibility toward another antibiotic. Cellular hysteresis increases bacterial extinction in fast sequential treatments and reduces selection of resistance by favoring responses specific to the induced physiological effects. Fast changes between antibiotics are key, because they create the continuously high selection conditions that are difficult to counter by bacteria. Our study highlights how an understanding of evolutionary processes can help to outsmart human pathogens.

Author contributions: R.R., D.I.A., and H.S. designed research; R.R., P.D., and C.B. performed research; R.R., C.S.G., P.R., and A.T. analyzed data; R.R., C.S.G., and A.T. developed and analyzed the mathematical model; R.R. and P.R. analyzed genomic data; and R.R., D.I.A., and H.S. wrote the paper.

The authors declare no conflict of interest.

This article is a PNAS Direct Submission. S.B. is a guest editor invited by the Editorial Board.

Data deposition: The sequences reported in this paper have been deposited in the NCBI Sequence Read Archive (SRA) database, https://www.ncbi.nlm.nih.gov/sra (Bioproject no. PRJNA484297).

[1]To whom correspondence should be addressed. Email: hschulenburg@evolbio.mpg.de.

This article contains supporting information online at www.pnas.org/lookup/suppl/doi:10.1073/pnas.1810004115/-/DCSupplemental.

The objectives of our study were to test the potential of negative hysteresis to enhance efficacy of sequential therapy. We used the pathogen *Pseudomonas aeruginosa* as a model—the second-most critical threat of a multidrug-resistant pathogen (18). We first characterized the hysteresis landscape for *P. aeruginosa* for three clinically relevant, bactericidal antibiotics with distinct cellular targets: ciprofloxacin (CIP), gentamicin (GEN), and carbenicillin (CAR). We then investigated how different levels of cellular hysteresis modulate the evolutionary adaptive response to sequential treatment using high-throughput experimental evolution, mathematical modeling, whole-genome sequencing, and functional genetic analysis of potential targets of selection. Finally, we validated the potential of antibiotic hysteresis for the inhibition and prediction of resistance evolution by second-order experimental evolution.

Results and Discussion

Cellular Hysteresis Depends on the Order of Drug Switches. We determined how short exposures to nonlethal concentrations of the three considered antibiotics CIP, GEN, and CAR affected later antibiotic treatment, by performing time-kill experiments (Fig. 1*A*). The inferred hysteresis landscape included negative, positive, and neutral effects and showed strong directionality. For the drug pair CAR/GEN, the sign of hysteresis effects was dependent on drug order (Fig. 1*B*): Preexposure to GEN, which is known to cause translational stress, protected cells from killing by CAR, while preexposure to CAR, which causes cell envelope stress, increased bactericidal activity of GEN (Fig. 1 *A*–*C* and Movie S1). Similar directionality was observed for the drug pair CIP/GEN (Fig. 1*B*). Neutral or mild hysteresis effects were observed for the pair CIP/CAR. Altogether, the hysteresis landscape indicated that population survival during the antibiotic switch is strongly history-dependent, thus emphasizing the importance of drug order for the design of effective treatment. Order dependence and the observation that negative hysteresis can be achieved with drug pairs known to interact either synergistically (GEN+CAR) or antagonistically (CIP+GEN) (19) demonstrate that hysteresis and drug interaction are not necessarily linked. Hysteresis is also distinct from collateral sensitivity, as it occurs immediately, i.e., without acquiring resistance mutations.

Further analysis of negative hysteresis caused by the CAR → GEN switch revealed that pretreatments as short as 15 min (equivalent to 1/3 generation time) and concentrations as low as 3 μg/mL [1/32 of the minimal inhibitory concentration (MIC)] were sufficient for the induction of accelerated killing (Fig. 1 *D* and *E*). Bactericidal activity increased 400-fold when the 15-min pretreatments were performed with higher concentrations, i.e., 2× MIC. These findings indicate a specific and robust physiological effect that may be exploited to increase the efficacy of antibiotic therapy, for example, by using sequential treatment. The increased killing is likely explained by β-lactam–induced acceleration of cellular influx of the aminoglycoside (20). The reduced killing in the reversed direction may be explained by aminoglycoside-induced up-regulation of efflux pumps (21, 22).

Negative Hysteresis Increases Treatment Efficacy and Constrains Evolution of Resistance. By modulating bacterial killing, we hypothesized that cellular hysteresis influences the rate of resistance evolution during sequential treatment dependent on drug order and the resulting cumulative level of hysteresis. To test these predictions, we conducted a high-throughput evolution experiment with 190 replicate populations over a total of 96 transfers (each with 12-h growth intervals; total of ∼500 generations; Fig. 2*A* and *SI Appendix*, Fig. S2). We included three main types of sequential protocols to disentangle the influence of hysteresis from the frequency and regularity of drug switches (Fig. 2*B*, columns 1–3). Evolutionary dynamics were tightly monitored, with continuous measurements of population growth (every 15 min). These measurements revealed that the evolutionary dynamics were separated into three main phases across the 96 transfers (Fig. 3*A*): (*i*) an initial phase up to roughly transfer 12, during which

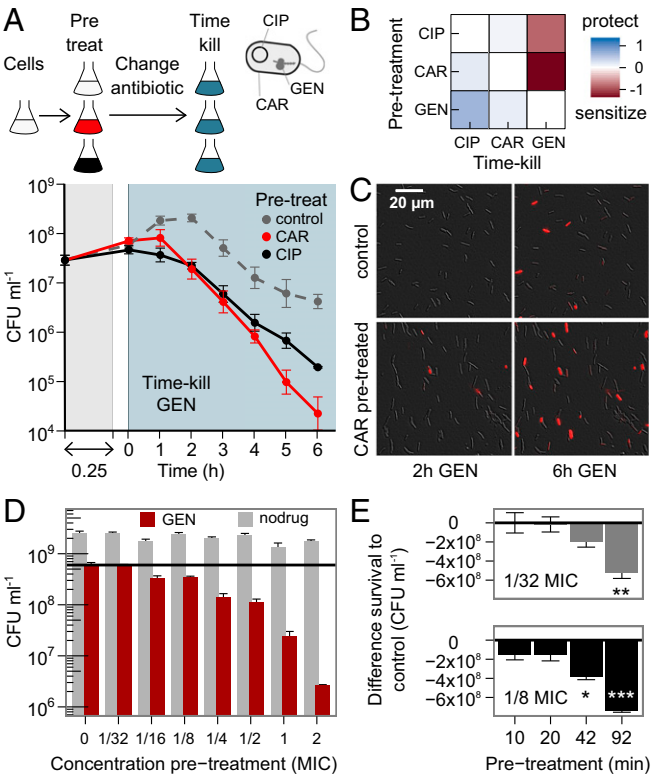

Fig. 1. Antibiotic-induced cellular hysteresis: Short antibiotic exposures affect later killing by other antibiotics. (*A*) Schematic and example data of time-kill experiment after pretreatment, using *P. aeruginosa* as model. Antibiotics CAR, CIP, and GEN have distinct cellular targets. Short pretreatments with nonlethal concentrations of CIP or CAR accelerate killing by GEN, shown as concentration of viable cells (cfu). Mean ± SEM, $n = 6$. (*B*) Antibiotic pretreatment sensitizes or protects bacteria during subsequent time-kill experiment with other antibiotics. (*C*) Time-lapse microscopy of control and CAR-pretreated bacteria during GEN treatment. Dead cells are stained red by propidium iodide. (*D*) Influence of CAR 15-min pretreatments with varying concentrations on survival in GEN, and drug-free media. Black line represents survival in GEN without pretreatment. (*E*) Subinhibitory antibiotic concentrations are sufficient to induce negative hysteresis, if pretreatments are sufficiently long (according to Student's *t* test, $n = 6$, $^{*}P < 0.05$, $^{**}P < 0.01$, $^{***}P < 0.001$).

populations adapted rapidly and treatments varied strongly in evolutionary dynamics; (*ii*) an optimization phase from transfer 12 up to approximately transfer 48, during which two treatments (monotherapy, slow regular protocol) were almost fully adapted, while the other two (fast regular and random protocols) still produced increases in growth, yet at lower rates as during the first phase; and (*iii*) the long-term dynamics from transfer 48 onward, during which only small growth increases and little variation among treatments were observed. For a more detailed analysis, we focused on the early dynamics up to transfer 12, because these encompass the strongest differences in the tested variables and cover a clinically relevant time period of 6 d.

For the early dynamics, fast and random sequences led to significant improvements in three independently characterized, complementary measures for treatment efficacy (Fig. 2*B*; see *SI Appendix*, Tables S1–S6 for statistics), including (*i*) higher extinction frequencies (inferred from absence of growth during experimental evolution), (*ii*) lower adaptation rates (calculated from growth characteristics measured during the evolution experiment), and (*iii*) lower levels of evolved multidrug resistance (MDR, determined from antibiotic dose–response curves for individual bacterial clones isolated from the evolving populations; *SI Appendix*, Fig. S3). Importantly, the cumulative

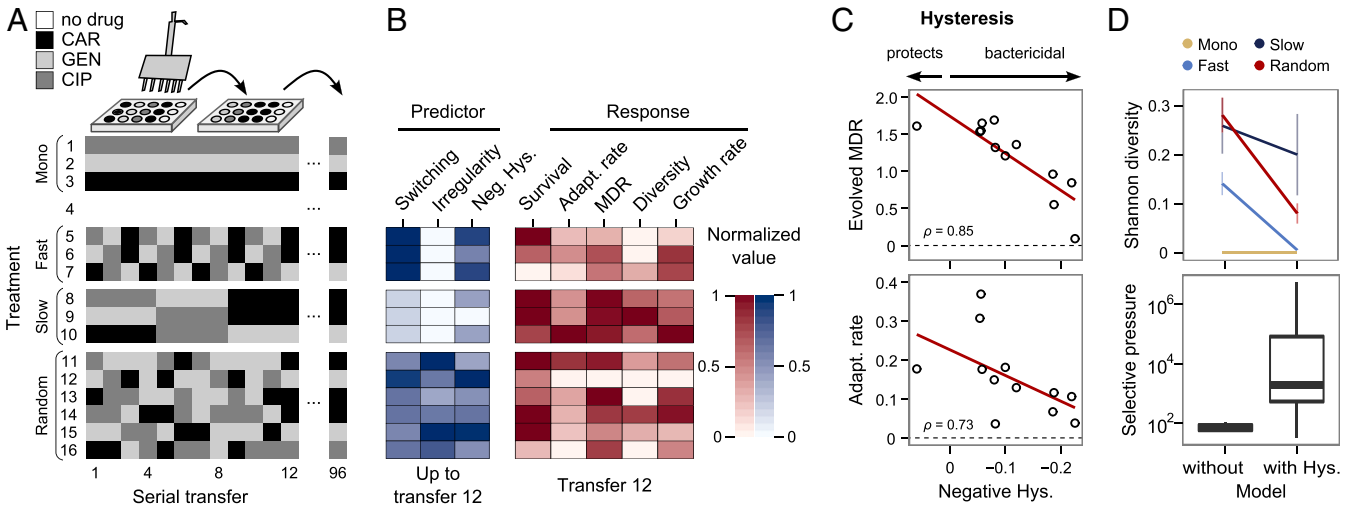

Fig. 2. Negative hysteresis can constrain the bacterial evolutionary response during sequential treatment. (*A*) Schematic of evolution experiment with three main types of sequential treatments plus controls, including a total of 16 individual protocols. Only the first 12 transfers are illustrated. (*B*) Variation in tested parameters and measured traits up to transfer 12. The tested parameters include cumulative levels of negative hysteresis (Neg. Hys., dark indicates high levels), switching rate, and regularity of change (dark indicates high irregularity). The evolutionary response was measured for population survival (max = 12), adaptation rate (Adapt. rate, $n \leq 12$, extinct lineages excluded), evolved MDR ($n = 35$), genotypic diversity ($n = 20$), and exponential growth rate in absence of drugs (weighted mean, $n = 3$). (*C*) Negative hysteresis levels (high levels toward right) correlated significantly with evolved MDR (red line shows regression line). (*D*) A mathematical model predicted lower genotypic diversity and higher selection intensities when accounting for cellular hysteresis.

levels of hysteresis were significantly correlated to both adaptation rates and evolved MDR (Spearman rank correlation, rho $\geq$ 0.73, $P \leq 0.01$; Fig. 2*C*). Evolved MDR was also significantly associated with switching rate, but to a lesser degree (Spearman rank correlation, rho = 0.66, $P = 0.019$), while there was no significant relationship between switching and adaptation rates (*SI Appendix*, Fig. S5). Increases in both negative hysteresis level and switching rate led to higher extinction frequencies, even though the effect was not statistically significant. We conclude that, even though switching rate is important, the consideration of negative hysteresis is sufficient to predict treatment efficacy.

Surprisingly, the fast sequential protocols resulted in significantly fewer resistance types and thus less genotypic diversity than the slow regular treatments (Figs. 2*B* and 3*B* and *SI Appendix*, Fig. S4 and Table S3). These findings contrast with expectations from population genetic theory, because fast switching should have prevented competitive exclusion and, instead, caused coexistence of multiple types that continuously varied in relative frequency parallel to antibiotic exposure. To assess these dynamics, we developed and analyzed a mathematical model tailored to the design of the evolution experiment. Under standard conditions (without hysteresis), the model indeed predicted coexistence of several types under fast sequential conditions (Fig. 2*D* and *SI Appendix*, Fig. S6). Importantly, when we added hysteresis effects to the model, we found increased selection pressure and a reduction of diversity, especially for the fast and random sequential protocols. These observations suggest that the inducible physiological effects act as a strong selective constraint during sequential treatment and influence diversity within the evolving populations.

The mathematical model indicated that negative hysteresis increases selection intensity (Fig. 2*D*), yet the observed outcome was not MDR—as would be expected from competitive release (23)—but rather a constrained ability to evolve MDR (Fig. 2*B*). Thus, we hypothesized that negative hysteresis selects for traits specifically directed against the inducible physiological effects rather than resistance. This idea was supported by our additional analysis of growth rate. Almost all drug protocols resulted in significantly reduced growth rates under drug-free conditions (Fig. 2*B*, last column), but the three sequences (#5, #12, #15) with high levels of negative hysteresis and almost no evolved MDR showed the strongest growth reductions of up to 41%. The combination of reduced growth and no MDR is indicative of antibiotic tolerance (24), an evolutionary strategy, in which bacteria evade killing by slow growth and which could have been favored through selection by negative hysteresis.

Negative Hysteresis Favors Genetic Changes Mediating Tolerance and an Unknown Response. To further assess the selective impact of negative hysteresis, we characterized the genes that have likely been the targets of selection using whole-genome sequencing and functional genetic analysis. The genomic characterization identified different sets of mutations to be favored by the main treatment types (Fig. 4 and Dataset S1). Intriguingly, the single nonresistant isolate from protocol #12 harbored a mutation that mediated a phenotypic response related to antibiotic tolerance. In detail, we followed concepts and methodology described previously (25), to test for tolerance with the help of time-kill experiments. These experiments revealed absence of resistance but reduced killing on all three antibiotics (Figs. 3*B* and 5*B* and *SI Appendix*, Table S7), consistent with antibiotic tolerance. This isolate had two mutations, a point mutation in the *ispA* gene (leading to amino acid change Y249D) and a frame shift in the *gcvT2* gene. Because the *gcvT2* mutation occurred across treatment groups (Fig. 4*A*), the *ispA* mutation is likely the adaptive change that caused reduced growth, possibly due to the toxic accumulation of isoprenyl diphosphates, as previously recorded for a Δ*ispA E. coli* mutant (26). Sequence #12 was enriched for CAR-induced sensitization toward GEN (Fig. 2*A*). A reassessment of the CAR → GEN transition showed that bacterial cells of this isolate could no longer be sensitized (Fig. 5*C*). We conclude that, in this single case, selection by negative hysteresis in sequence #12 has likely been countered by the emergence of a process related to antibiotic tolerance, mediated through a mutation in *ispA*.

In several other fast sequential protocols, negative hysteresis was countered by mutations in *cpxS* (*SI Appendix*, Fig. S7). This gene is related to the *E. coli* envelope stress response system CpxA–CpxR, which is activated by misfolded proteins, as caused by aminoglycosides (27), and involved in intrinsic resistance to these drugs in *E. coli* (28). Mutations in *cpxS* were significantly enriched in fast sequential treatments (*SI Appendix*, Table S6), including those with little indication of antibiotic tolerance (e.g., normal growth under drug-free conditions; protocol #7; Fig. 2*B*). To explore its function, we reintroduced one prevalent *cpxS*

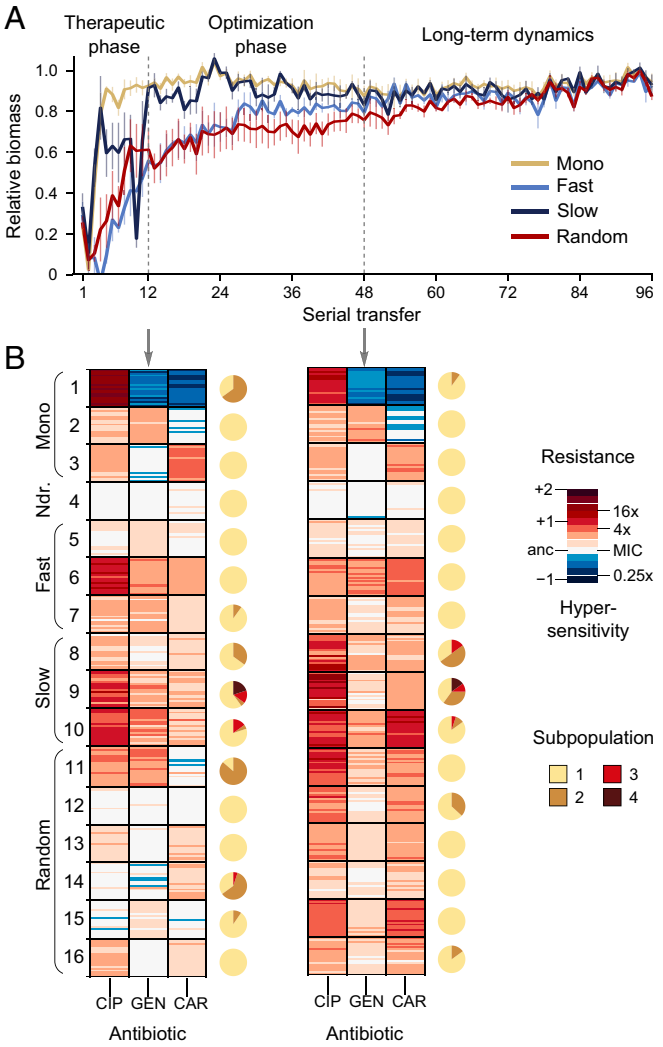

Fig. 3. Overall evolutionary dynamics in response to sequential treatment. (*A*) Evolutionary dynamics expressed as total growth relative to evolving untreated controls. Mean ± 2 SEM, $n = 3$ to 6 protocols per treatment with 12 replicate populations, extinct lineages excluded. Dashed vertical lines indicate time points for isolation of evolved bacterial clones. (*B*) Resistance profiles of 320 clones isolated after transfer 12 from 16 populations (early isolates) and 320 clones isolated after transfer 48 (late isolates); the clones are indicated by bars within the boxes for a particular treatment. Pie charts indicate frequencies of phenotypic subpopulations, as determined by hierarchical clustering. Different colors denote the distinct types per population. Summary statistics are presented in Fig. 2.

mutation (leading to T163P) into the ancestral background and compared it to the ancestor and the similarly generated *mexR* (T130P) mutant as a control. MexR regulates the multidrug efflux pump MexAB-OprM, which can extrude different drug classes (29), potentially conferring MDR. *MexR* mutations are unlikely favored by negative hysteresis, as this gene was frequently and exclusively mutated in slow sequential treatments (Fig. 4*A*). Our analysis revealed that resistance against CIP and CAR was moderate for the *cpxS* mutant, but strongly increased for the *mexR* mutant, while neither mutation altered resistance to GEN (Fig. 5*A* and *SI Appendix*, Fig. S8). Importantly, using two independent methods, we consistently found that the CAR-induced sensitization toward GEN was abolished in the *cpxS* mutant, but still present in the *mexR* mutant (Fig. 5*C*), which is also consistent with growth rate dynamics in the evolution experiment (*SI Appendix*, Fig. S9). In conclusion, mutations in *cpxS* were favored in several fast sequential protocols and are thus likely to represent a general response to selection by negative hysteresis, apparently independent of antibiotic tolerance.

The above result for the *mexR* mutant additionally suggests that canonical resistance mechanisms do not abolish negative hysteresis. To further test this point, we characterized CAR → GEN hysteresis for defined mutants in *mexA*, *nalC*, and *nalD*, all affecting the MexAB-OprM multidrug efflux system. Despite their increased resistance to the antibiotic of the pretreatment (i.e., CAR), negative hysteresis and thus enhanced killing by GEN could be readily induced, with high (up to 600 μg/mL) and also subinhibitory doses (*SI Appendix*, Fig. S10). We conclude that bacteria can suffer from negative hysteresis even if they are resistant against the drug of the sensitizing pretreatment.

An Independent Experimental Test Validates the Importance of Negative Hysteresis. To specifically test the consequences of negative hysteresis, we took inspiration from Lewontin's theoretical work on evolutionary historicity (30), which highlighted that the order of events influences the evolutionary outcome. We thus repeated evolution experiments with the reversed order of drugs for the most effective sequence, #12, and the least effective sequence, #13 (inferred from evolved MDR; Fig. 2*B*). The reverse sequences had the same drug proportions and number of switches as the original sequences, but the direction of transitions was opposite. As a consequence, all was equal except that the cumulative level of negative hysteresis was decreased by 10% in the first case and increased by 11% in the second case (Fig. 6*A*). As expected, reversing #12 decreased extinction frequency (Fig. 6*B*) and significantly increased resistance (Fig. 6*C* and *SI*

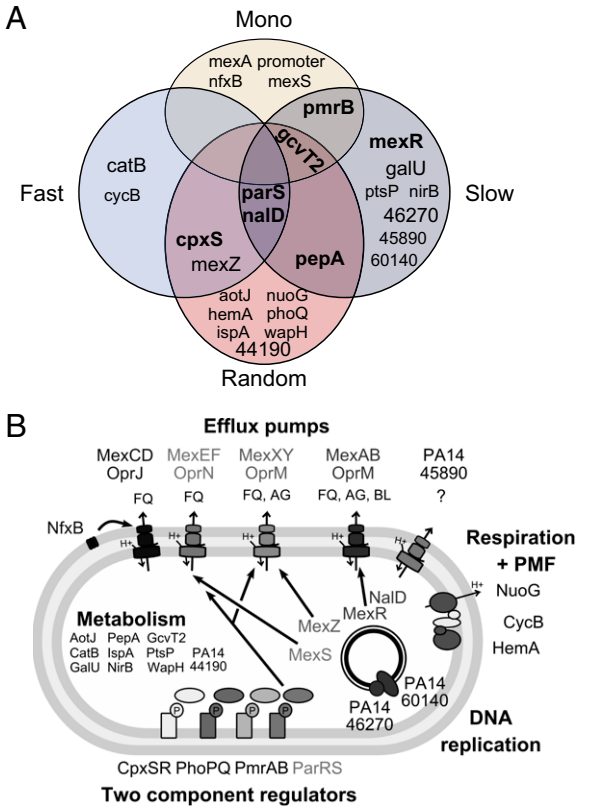

Fig. 4. Genetic basis of adaptation. (*A*) Overlap of mutated genes among treatment types. Typeface and boldness indicate number of mutations in a gene. (*B*) Schematic of cellular functions targeted by adaptive evolution. Resistance is mostly achieved by mutations in two-component regulators or transcriptional regulators that control efflux pumps. AG, aminoglycosides; BL, β-lactams; FQ, fluoroquinolones; PMF, proton motive force.

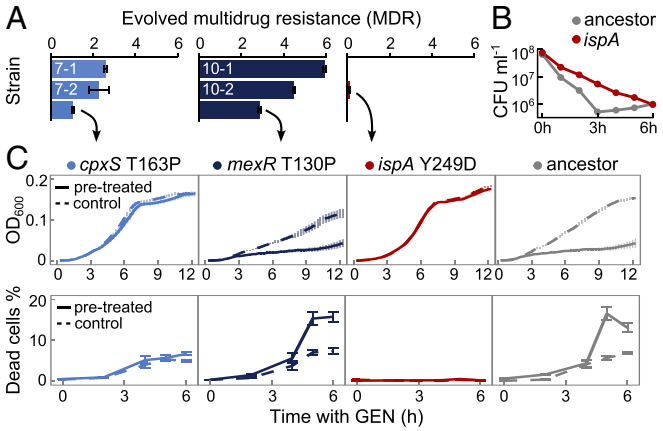

Fig. 5. Evolutionary adaptation to negative hysteresis. (*A*) Evolved MDR of isolates from sequential treatments (top two bars) and corresponding reconstructed mutants (bottom bar). Mean ± SEM, $n \geq 6$. (*B*) Isolate from sequential protocol #12 with mutation in *ispA* shows antibiotic tolerance and thus reduced cellular death during antibiotic exposure (in this case, CIP). (*C*) (*Top*) CAR-induced sensitization toward GEN (solid lines) inhibited growth in ancestor and *mexR* mutant but neither *cpxS* nor *ispA* mutants. Mean ± SEM, $n = 6$. (*Bottom*) Confirmation of results by measuring dead cells over time using flow cytometry. Mean ± SEM, $n = 3$.

Appendix, Table S7). Conversely, reversing #13 increased extinction, although resistance was not affected, most likely because only few populations survived and could be used for resistance analysis. These results demonstrate that cellular hysteresis can determine the efficacy of sequential therapy.

Conclusions

Our results show that antibiotics can induce long-lasting changes in bacterial physiology that enhance or inhibit the bactericidal activity of other antibiotics, thereby revealing a principle, cellular hysteresis, that can be exploited to optimize antibiotic therapy. Cellular hysteresis can still act in bacteria that are resistant against the pretreatment drug, highlighting its clinical potential, where antibiotic resistance is widespread. Fast switching between antibiotics is key, because it can increase the cumulative effect of negative hysteresis, leading, in our experiments, to improvements in three complementary measures of treatment efficacy. Negative hysteresis exerted specific selection that did not favor resistance mutations, but rather mutations that counter the inducible physiological effects, such as those identified here for *ispA* and *cpxS*. We also showed that slow drug changes enhance resistance evolution and target different sets of genes. Our findings may thus explain the limited success of antibiotic cycling in the clinic, where antibiotics are usually changed once per month or less often (31). Negative hysteresis may further explain the particular success of one of the very few clinical studies with one antibiotic switch in less than a day. This study from 1988 demonstrated that the staggered application of first a β-lactam and then, 4 h later, an aminoglycoside—exactly the switch required for negative hysteresis—causes a significant reduction and often full clearance of *P. aeruginosa* from the lungs of a small cohort of cystic fibrosis patients (32). In this particular study, clearance could not be achieved by the corresponding combination treatment [i.e., simultaneous dosing (32)]. In our own previous work, the CIP+GEN combination did not produce any clearance, while the CAR+GEN combination at equivalent effective dose led to clearance rates comparable to those observed here for sequential treatments with high levels of negative hysteresis (19), generally supporting the possible power of temporal changes for effective treatment. Novel approaches such as multilayer liposomes (33) may then become useful for sequential drug delivery. A further exploration of inducible physiological effects may thus help to find new ways for improving antibiotic therapy—using the available drugs in a rational and refined way.

Materials and Methods

Material. *P. aeruginosa* UCBPP-PA14 (34) was grown at 37 °C in M9 medium supplemented with glucose (2 g/L), citrate (0.5 g/L), casamino acids (1 g/L), and an antibiotic, as indicated.

Time-Kill Experiments. Exponential phase cells (5×10^7 cfu/mL) were pretreated with sublethal antibiotic concentrations for the indicated time. The medium was exchanged to expose cells to a second antibiotic at IC_{75}, followed by cfu counting for 6 h. Hysteresis effects were quantified as the average $\log_{10}$ difference in cfu counts of pretreated and control cultures. Negative values indicate sensitization, and positive values indicate protective effects. Bacterial killing was confirmed by time-lapse microscopy, monitoring bacteria on agarose pads (35) using a Zeiss LSM 700.

Dose–Response Curves. A standardized inoculum (5×10^5 cfu) was incubated with defined antibiotic concentrations in 96-well plates for 12 h at 37 °C, followed by optical density measurements at 600 nm (OD_{600}).

Main Evolution Experiment. We performed serial dilution evolution experiments (6, 23, 36) and selection with 16 different antibiotic sequences (see also *SI Appendix*). Sequences #1 to #4 had constant environments. Sequences #5 to #16 contained equal frequencies of CIP, GEN, and CAR, but differed in hysteresis levels, due to drug order and switching rate. Each treatment had 12 replicates (founded with 5×10^5 cells from six independent PA14 starting cultures) and 96 serial transfers (2% transfer volume), each separated by 12 h. Antibiotic selection was applied at IC_{75} in 96-well plates, and growth was monitored by OD_{600} every 15 min (EON; BioTek Instruments; 180-rpm double orbital shaking). Evolved material was conserved at −80 °C in 10% (vol/vol) DMSO. Resistance evolution was assessed using the integral of the growth curve divided by the integral for the untreated reference evolving in parallel (relative area under curve or relative biomass, Fig. 3). Low values denote sensitivity to treatment, a value of 1 uninhibited growth (dynamics for all populations are shown in *SI Appendix*, Fig. S11). Adaptation rate was calculated with a sliding window approach as X^{-1}, where X is the transfer at which the mean relative biomass of a sliding window of 12 transfers reaches 0.75 for the first time. This measure is comparable with the previously described rate of adaptation (36), defined for constant environments, yet not applicable to fluctuating environments, in which growth often oscillates. Extinction frequencies were determined at the end of the evolution experiment by counting cases unable to grow in drug-free media.

Characterization of Evolved Isolates. We measured antibiotic dose–response curves for 880 evolved isolates from evolved populations after transfers 12 and 48. Resistance profiles were obtained as in *Dose–Response Curves*, with concentrations from 1/8 MIC to 16× MIC, assessed as the relative area of dose–response curves for isolates and corresponding ancestors measured on the same plate (*SI Appendix*, Fig. S3). For treatment comparisons, we defined MDR scores as the sum of resistance values on the three antibiotics. Subpopulations were identified by hierarchical clustering of resistance profiles. We characterized growth in drug-free medium. See *SI Appendix*.

Mathematical Model. We developed a deterministic model to explore the ability of different antibiotic protocols to limit population growth by the evolution of

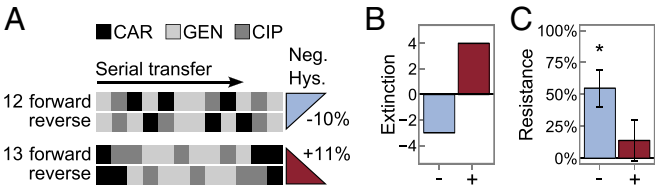

Fig. 6. Reversal of sequential protocols predictably altered treatment efficacy due to changes in negative hysteresis levels. (*A*) Reversal of the first 12 steps in two sequential treatments changed the overall level of negative hysteresis. (*B*) Change of negative hysteresis predictably altered extinction frequencies. (*C*) Decreasing negative hysteresis levels significantly increased antibiotic resistance in surviving lineages (according to post hoc test, generalized linear mixed model, $n = 3$, $^*P < 0.05$). Mean ± SEM.

resistant types. We modified a logistic growth model (competition for space) that included mutation, $\dot{x}_i = (r_i x_i + \sum_{j=1}^{n}(q_{ji} r_j x_j - q_{ij} r_i x_i))[1 - (1/K)\sum_{l=1}^{n} x_l]$. Different genotypes were included with density x_i and growth rate r_i. Each genotype had three growth rates, for each of the possible treatments, $r_i = \{r_i^{CIP}, r_i^{GEN}, r_i^{CAR}\}$. The mutation rate q_{ji} determined the change of genotype j to another genotype i. The carrying capacity was defined by K. To simulate serial transfers, the mixture of types was diluted by a dilution factor DF at the end of each season. If the density of a genotype fell below the cutoff κ during dilution, it was lost and could only reappear via mutation. Following dilution, treatments could either switch or be repeated. The model was parameterized according to the evolution experiment: $K = 10^8$ cells, $DF = 50$ applied every 12 h, $\kappa = 10$. Population size was $K/4$ (IC_{75}) directly before the first transfer. Growth dynamics were generated for a simple system with four competing genotypes, the nonresistant wt and three mutants, individually resistant to CIP, GEN, or CAR, parameterized according to the results of the monotreatments #1 to #3 (growth rate table R, *SI Appendix*, Fig. S6). Some mutant growth rates were lower than those of the wt on particular antibiotics, denoting collateral sensitivity, consistent with previous results (37). Switches between antibiotics allowed for hysteresis effects, which we included by multiplying the respective growth rates from table R with the corresponding entry from table S, showing the antibiotic-induced physiological effects, experimentally inferred for the four genotypes (*SI Appendix*, Fig. S6). Using this model, we generated growth dynamics for mixed populations for the different sequential treatments, either with or without hysteresis. From the modeled dynamics, we inferred the selective pressure, as defined by K/x_{wt}, and the within-population diversity, as calculated from Shannon entropy.

Genomics and Functional Genetic Analysis. Whole-genome sequencing was performed for 30 evolved isolates from different subpopulations at the early time point, and the three subpopulations of #8 at the late time point (*SI Appendix*). For defined mutants (*SI Appendix*), we assessed the change in growth upon pretreatment by OD_{600} every 15 min. We additionally used flow cytometry (Guava EasyCyte HT Blue-Green; Merck KGaA) with hourly samples, Live/Dead staining, and three technical replicates. For staining, cells were incubated for 10 min with propidium iodide (P4170-25MG; Sigma-Aldrich) and thiazole orange (390062-250MG; Sigma-Aldrich). We assessed antibiotic tolerance for isolate 12-1a-E2-4 (isolated after transfer 12 from sequence #12) via minimal duration of killing (25).

Replay Evolution Experiment. The experiment was performed as the main evolution experiment, using sequences #12, #12rev, #13, #13rev, and an untreated control. Sequences #12 and #13 were the same as the first 12 transfers in the main experiment, and #12rev and #13rev were their respective reverse sequences. Resistance was quantified by the fold changes in IC_{75}.

Statistical Analyses. Data analysis was performed with *R* (38). Statistics, *P* values, and explanatory notes are provided in *SI Appendix*, Tables S1–S6.

Data Availability. The data are supplied as Datasets S1–S5. Sequence data are available from NCBI, BioProject PRJNA484297.

ACKNOWLEDGMENTS. We thank T. Bollenbach, T. Dagan, C. Eschenbrenner, D. Falush, M. Habig, A. Read, J. Rolff, M. Sixt, and the H.S. lab for advice; and G. Hemmrich-Stanisak, T. Naujoks, C. Noack, and M. Vollstedt from the Institute of Clinical Molecular Biology for DNA sequencing, as supported by the German Science Foundation Cluster of Excellence EXC 608. This research was funded by the German Science Foundation Grant SCHU 1415/12 (to H.S.), a Young Scientist Grant from the Zentrum Molekulare Biowissenschaften Kiel (to R.R.), the International Max Planck Research School for Evolutionary Biology (R.R.), the Swedish Research Council (D.I.A.), the Leibniz Science Campus EvoLUNG (H.S.), and the Max-Planck Society (C.S.G., A.T., and H.S.).

1. Bürger R, Lynch M (1995) Evolution and extinction in a changing environment: A quantitative-genetic analysis. *Evolution* 49:151–163.
2. Carroll SP, et al. (2014) Applying evolutionary biology to address global challenges. *Science* 346:1245993.
3. Liu Y-Y, et al. (2016) Emergence of plasmid-mediated colistin resistance mechanism MCR-1 in animals and human beings in China: A microbiological and molecular biological study. *Lancet Infect Dis* 16:161–168.
4. Bloemberg GV, et al. (2015) Acquired resistance to bedaquiline and delamanid in therapy for tuberculosis. *N Engl J Med* 373:1986–1988, and erratum (2015) 375:e29.
5. Kim S, Lieberman TD, Kishony R (2014) Alternating antibiotic treatments constrain evolutionary paths to multidrug resistance. *Proc Natl Acad Sci USA* 111:14494–14499.
6. Roemhild R, Barbosa C, Beardmore RE, Jansen G, Schulenburg H (2015) Temporal variation in antibiotic environments slows down resistance evolution in pathogenic *Pseudomonas aeruginosa*. *Evol Appl* 8:945–955.
7. Fuentes-Hernandez A, et al. (2015) Using a sequential regimen to eliminate bacteria at sublethal antibiotic dosages. *PLoS Biol* 13:e1002104.
8. Yoshida M, et al. (2017) Time-programmable drug dosing allows the manipulation, suppression and reversal of antibiotic drug resistance in vitro. *Nat Commun* 8:15589.
9. Szybalski W, Bryson V (1952) Genetic studies on microbial cross resistance to toxic agents. I. Cross resistance of *Escherichia coli* to fifteen antibiotics. *J Bacteriol* 64: 489–499.
10. Imamovic L, Sommer MOA (2013) Use of collateral sensitivity networks to design drug cycling protocols that avoid resistance development. *Sci Transl Med* 5:204ra132.
11. Linares JF, Gustafsson I, Baquero F, Martinez JL (2006) Antibiotics as intermicrobial signaling agents instead of weapons. *Proc Natl Acad Sci USA* 103:19484–19489.
12. Hoffman LR, et al. (2005) Aminoglycoside antibiotics induce bacterial biofilm formation. *Nature* 436:1171–1175.
13. VanBogelen RA, Neidhardt FC (1990) Ribosomes as sensors of heat and cold shock in *Escherichia coli*. *Proc Natl Acad Sci USA* 87:5589–5593.
14. Lambert G, Kussell E (2014) Memory and fitness optimization of bacteria under fluctuating environments. *PLoS Genet* 10:e1004556, and erratum (2014) 10:e1004556.
15. Ram S, Goulian M (2013) The architecture of a prototypical bacterial signaling circuit enables a single point mutation to confer novel network properties. *PLoS Genet* 9: e1003706.
16. Lazim Z, Humphrey TJ, Rowbury RJ (1996) Induction of the PhoE porin by NaCl as the basis for salt-induced acid sensitivity in *Escherichia coli*. *Lett Appl Microbiol* 23: 269–272.
17. Veening J-W, Smits WK, Kuipers OP (2008) Bistability, epigenetics, and bet-hedging in bacteria. *Annu Rev Microbiol* 62:193–210.
18. World Health Organization (2017) Global priority list of antibiotic-resistant bacteria to guide research, discovery, and development of new antibiotics. Available at www.who.int/en/news-room/detail/27-02-2017-who-publishes-list-of-bacteria-for-which-new-antibiotics-are-urgently-needed. Accessed May 16, 2017.
19. Barbosa C, Beardmore R, Schulenburg H, Jansen G (2018) Antibiotic combination efficacy (ACE) networks for a *Pseudomonas aeruginosa* model. *PLoS Biol* 16:e2004356.
20. Plotz PH, Davis BD (1962) Synergism between streptomycin and penicillin: A proposed mechanism. *Science* 135:1067–1068.
21. Hay T, Fraud S, Lau CH-F, Gilmour C, Poole K (2013) Antibiotic inducibility of the mexXY multidrug efflux operon of *Pseudomonas aeruginosa*: Involvement of the MexZ anti-repressor ArmZ. *PLoS One* 8:e56858.
22. Morita Y, Sobel ML, Poole K (2006) Antibiotic inducibility of the MexXY multidrug efflux system of *Pseudomonas aeruginosa*: Involvement of the antibiotic-inducible PA5471 gene product. *J Bacteriol* 188:1847–1855.
23. Pena-Miller R, et al. (2013) When the most potent combination of antibiotics selects for the greatest bacterial load: The smile-frown transition. *PLoS Biol* 11:e1001540.
24. Fridman O, Goldberg A, Ronin I, Shoresh N, Balaban NQ (2014) Optimization of lag time underlies antibiotic tolerance in evolved bacterial populations. *Nature* 513:418–421.
25. Brauner A, Fridman O, Gefen O, Balaban NQ (2016) Distinguishing between resistance, tolerance and persistence to antibiotic treatment. *Nat Rev Microbiol* 14:320–330.
26. Fujisaki S, et al. (2005) Disruption of the structural gene for farnesyl diphosphate synthase in *Escherichia coli*. *J Biochem* 137:395–400.
27. Davis BD, Chen LL, Tai PC (1986) Misread protein creates membrane channels: An essential step in the bactericidal action of aminoglycosides. *Proc Natl Acad Sci USA* 83: 6164–6168.
28. Guest RL, Raivio TL (2016) Role of the Gram-negative envelope stress response in the presence of antimicrobial agents. *Trends Microbiol* 24:377–390.
29. Masuda N, et al. (2000) Substrate specificities of MexAB-OprM, MexCD-OprJ, and MexXY-oprM efflux pumps in *Pseudomonas aeruginosa*. *Antimicrob Agents Chemother* 44:3322–3327.
30. Lewontin RC (1967) The principle of historicity in evolution. *Wistar Inst Symp Monogr* 5:81–94.
31. Abel zur Wiesch P, Kouyos R, Abel S, Viechtbauer W, Bonhoeffer S (2014) Cycling empirical antibiotic therapy in hospitals: Meta-analysis and models. *PLoS Pathog* 10: e1004225.
32. Guggenbichler JP, Allerberger F, Dierich MP, Schmitzberger R, Semenitz E (1988) Spaced administration of antibiotic combinations to eliminate *Pseudomonas* from sputum in cystic fibrosis. *Lancet* 2:749–750.
33. Morton SW, et al. (2014) A nanoparticle-based combination chemotherapy delivery system for enhanced tumor killing by dynamic rewiring of signaling pathways. *Sci Signal* 7:ra44.
34. Rahme LG, et al. (1995) Common virulence factors for bacterial pathogenicity in plants and animals. *Science* 268:1899–1902.
35. Young JW, et al. (2011) Measuring single-cell gene expression dynamics in bacteria using fluorescence time-lapse microscopy. *Nat Protoc* 7:80–88.
36. Hegreness M, Shoresh N, Damian D, Hartl D, Kishony R (2008) Accelerated evolution of resistance in multidrug environments. *Proc Natl Acad Sci USA* 105:13977–13981.
37. Barbosa C, et al. (2017) Alternative evolutionary paths to bacterial antibiotic resistance cause distinct collateral effects. *Mol Biol Evol* 34:2229–2244.
38. R Core Team (2016) R: A Language and Environment for Statistical Computing (R Foundation for Statistical Computing, Vienna), R Version 3.3.1. Available at www.R-project.org/. Accessed June 21, 2016.